Oxidation catalysis on Pt and Au : complexity of simple chemistry

Spronsen, M.A. van

Chapter 4

High-pressure operando STM studies giving insight in CO oxidation and NO reduction over Pt(110)

4.1 Introduction

Much of our current knowledge of the precise mechanisms underlying chemical reactions at catalytic surfaces is derived from experiments under UHV or high vacuum (HV) conditions. This discrepancy with respect to the typical working conditions of practical catalysts (i.e., high pressure (HP) and elevated temperatures) comes from the fact that many surface sensitive techniques such as LEED, AES, and XPS cannot be easily combined with the environment to which a catalyst would normally be exposed. Typical examples of catalysis would be the three-way catalyst in an automotive exhaust system, or catalytic processes in the petrochemical industry. Moreover, UHV conditions provide a clean and easily controllable environment for accurate experiments [114, 115]. Although such low-pressure model studies have contributed extensively to our fundamental understanding of catalysts, recent investigations at high gas pressures have yielded new insight that goes beyond the mere extrapolation of the low-pressure results [21, 116–118]. This difference is often referred to as the "pressure gap" [119, 120]. Recently, several surface analysis techniques have been adapted to realistic conditions. Examples are TEM [121], SXRD [122], STM [20, 120, 123], and AFM [22].

Scanning tunneling microscopy is one of the few atomically sensitive surface science techniques that do not introduce fundamental problems or limitations when bridging the pressure gap. This technique can operate in the full range from UHV to HP of, e.g., 1 bar and beyond, and from cryogenic temperatures to temperatures well above 1000 K [124, 125]. With its capability to image surfaces with atomic resolution, STM holds the promise to determine the detailed dependence of the structure of a model catalyst's surface on various gas environments, to identify the active sites for catalytic reactions, and to elucidate the role of possible promoters, all under the relevant, high-pressure, high-temperature conditions of the catalytic processes of interest. The weak, local interaction of the tip with the surface provides confidence that in most cases this interaction will not significantly affect the structure and the properties of the catalyst. These advantageous properties of the technique go hand-in-hand with a demanding combination of technical difficulties, involving, e.g., the imaging stability of the instrument in terms of drift and noise resulting from temperature and pressure variations, and from the presence of a gas flow. In addition, the signal-to-noise ratio in the detection of the reaction products in the gas mixture is demanding as well.

In order to investigate the relationship between surface structure and activity of a catalyst under industrially relevant conditions, we have developed the ReactorSTM system [19]. This system combines a small flow reactor, integrated with STM into a UHV system that is equipped with standard, high-quality surface preparation and analysis techniques, such as ion bombardment, metal deposition, XPS, AES, and LEED. The architecture of the system is such that the sample can be transported from the various sample preparation and analysis tools into the ReactorSTM without breaking the UHV conditions. During the HP STM experiments, the UHV stays uncompromised even at pressures inside the reactor well above 1 bar. The flow-reactor geometry and the special design of the low-volume, high-purity gas supply system allows us to continuously control the gas composition in the reactor, the flow rate, and the reactor pressure, and it allows for rapid, time-resolved analysis on the gas effluent from the reactor during STM

imaging, without the need to retract the tip, which would result in a 'blind moment'. In this way, the system enables us to study the surface structure of an active catalyst with atomic resolution, combined with simultaneous reactivity measurements. Thereby, we can directly correlate structural changes with chemical activity. The system is a strongly improved version of the prototype that we reported on earlier [20, 21] and a commercial version has been developed by Leiden Probe Microscopy BV [42]. In this chapter, we report on the first results from this new instrument applied to two different catalytic reactions, both on the Pt(110) surface: CO oxidation and NO reduction. CO oxidation is one of the reactions occurring in the catalytic cleaning of exhaust gases from automotive engines. Selective oxidation of CO to CO_2 has also received major attention in order to clean H_2 streams for fuel cells [126]. Typical catalysts used for this reaction include the noble metals, such as Pt [127]. The (110) surface of Pt is perhaps the best studied surface after Pt(111) for the oxidation of CO. Early studies of this reaction system have revealed highly interesting phenomena, such as, kinetic oscillations [128] and reaction induced faceting [129]. However, these phenomena were observed in a pressure range from high vacuum to UHV and using traditional surface science techniques. This experimental window in which detailed information of the surface can be obtained has been dramatically increased by the recent developments of in situ and operando techniques. Because of the interesting discoveries obtained in vacuum, it is easy to understand that this surface received much attention from researchers using these newly developed techniques. One of the key questions is whether the behavior observed under vacuum conditions can be extrapolated to real reaction conditions and which new surprises can be found on the other side of the pressure gap.

High-pressure STM [21] and SXRD combined with DFT [116] have revealed the appearance of new surface structures and compositions, depending on the gas composition. Two of these structures are oxidic in nature. One is a surface oxide probably stabilized by carbonate ions and oxygen atoms. This oxide is observed when the ratio between the partial pressures of CO and O_2 is not too low. The other oxidic structure is a thin film of bulk-like α-PtO_2 and is formed at lower CO to O_2 partial-pressure ratios. Interestingly, both oxides show a higher reactivity towards CO oxidation compared to the metallic surface. The formation of α-PtO_2 and the reactivity to CO has been confirmed by one near-ambient-pressure XPS study [59], while a second study at slightly different pressure and gas compositions compared to the STM and SXRD studies showed only the metallic surface [130]. In addition to the surface oxide observed by SXRD, a different structure has been observed in which O atoms bind to the fcc hollow sites of a reconstructed (1×2)-Pt(110) surface. In this surface oxide, the O-atom-induced stress leads to the ejection of Pt atoms in a highly ordered manner, so that a Pt(110)-(12×2)-2O structure is adopted [62]. However, DFT combined with ab initio thermodynamics predicts that this surface oxide is not stable under reaction conditions [68, 110].

The oxidation of CO by O_2 serves as a 'model system' to demonstrate the improved resolution of the ReactorSTM under catalytic conditions.

The second part of this work describes experiments on the interaction between NO and H_2 and the Pt(110) surface. These interactions are key factors in understanding the selective reduction of NO, which is an extremely important process to clean exhaust gases of engines and large turbines. In contrast to the oxidation of CO, there is hardly

any in situ or in operando result reported on the reduction of NO. Previous work from our group shows that results obtained under reaction conditions strongly differ from the results obtained in UHV on the reaction between NO and CO on Pt(100) [131].

Different reducing agents can be used for this reaction, such as unburned fuel remains, CO and H_2. Hydrogen can be formed in exhaust gases by a water-gas shift reaction (equation 4.1) or via steam reforming with for example methane (equation 4.2).

$$CO + H_2O \rightarrow CO_2 + H_2 \tag{4.1}$$

$$CH_4 + H_2O \rightarrow CO + 3H_2 \tag{4.2}$$

4.2 Experimental

The results presented in this chapter have all been obtained with the ReactorSTM [19] and establish the first scientific output of this unique system, which is an improved version of the HP STM described by Rasmussen et al. [20]. Herbschleb et al. describe the ReactorSTM in full detail elsewhere [19]. Therefore, we only summarize the most important features of the system. The ReactorSTM is a flow cell integrated with an STM setup inside a UHV system. Only a few parts of the microscope are exposed to the reactive gases, i.e., the tip and a slider that form part of the microscope's coarse approach mechanism. Most parts of the microscope, such as the piezo tube, are outside the flow cell.

The combination between a UHV system and a flow cell gives the best of both worlds, fundamental surface science and the more applied catalytic research. We can use model catalysts and obtain a very clean and controlled starting point for the high-pressure experiment. Because we use a small flow reactor instead of backfilling a large-volume chamber, we can measure the reactivity with a much lower detection limit and higher time resolution. This reactivity is measured by leaking a small fraction of the gas from the reactor into a separate UHV chamber, housing a quadrupole mass spectrometer (QMS).

The Pt(110) sample, which was spark cut and polished to within 0.1° from the (110) plane [41], was cleaned with repetitive Ar^+ sputtering and annealing in UHV, at temperatures between 900–1100 K before every experiment. This procedure was complemented with an anneal step at 800 K in an O_2 atmosphere (pressure of $1\times10^{-(8-7)}$ mbar) to remove residual C. The removal of C and other impurities was checked with AES, until the peaks corresponding to impurities were on the level of the noise. In addition to the surface purity, LEED was used to determine the surface structure. The crystal was cleaned until LEED showed a well-defined (1×2) reconstruction. This reconstruction, the missing-row reconstruction, is known to occur on the clean (110) surfaces of Ir, Au, and Pt under UHV conditions [132]. The well-known distances of 0.78 nm [133] between the missing rows of the clean Pt(110)-(1×2) surface in UHV have been used to calibrate the in-plane displacement of the piezo tube scanner of the microscope. Monoatomic steps of the Pt(110) surface have been used to calibrate the vertical direction.

In order to start a high-pressure experiment, the sample must be transferred to the reactor. The sample itself forms the top wall of the reactor and is pressed onto the

reactor body, which holds the STM tip and the electrical connection from the tip to the STM preamplifier. The sample is sealed on the reactor with a fluoroelastomer[1] O-ring, forming a high-pressure/vacuum barrier that allows to maintain UHV conditions in the STM chamber and a pressure in the reactor of up to 6 bar. After the sample is pressed on the reactor, the reactor volume is no longer being pumped until the high-pressure gas flow is admitted. The pressure in the stage between UHV sample cleaning and the starting of the high-pressure experiment is solely determined by outgassing of the fluoroelastomer and other polymer parts, which is roughly estimated to be lower than 1×10^{-5} mbar. This outgassing is both temperature and time dependent with possibly some memory effects occurring between experiments. However, careful baking of the entire reactor should minimize crosstalk between experiments.

Recently, we have implemented a new configuration in which two small pumping lines have been constructed to maintain some pumping of the reactor volume by the UHV chamber in the time lag between UHV and HP conditions. This improved configuration has been used for the NO and H_2 exposure experiments reported here. Before the STM experiment can start, a coarse approach needs to be employed to bring the tip within tunneling distance of the surface. Since there is no optical access to the STM when the reactor is closed, this coarse approach must bridge a few millimeters and roughly takes between 20 and 60 minutes. To keep the sample as clean as possible one needs to question whether it is better to approach in a vacuum determined by outgassing and low pumping speed or to expose the sample directly to a flow of high-pressure inert gases.

When flowing high pressure of a gas mixture, the contamination is limited by the impurity level in the gas feed. The used gases all have typical purities of 6.0N, which corresponds to an impurity level of 1 ppm. This impurity level corresponds to a partial pressure of 1×10^{-3} mbar at a total pressure of 1 bar. However, having a gas flow through the reactor has the advantage that partial pressures of impurities outgassing from the polymer components are reduced to lower levels.

To start a high-pressure experiment with a sample that resembles the well-prepared UHV sample as closely as possible, it was found that it was best to execute the coarse approach step before introducing the gas flow.

Mechanically cut Pt/Ir tips have been used in the CO oxidation experiments without any in situ pretreatment. On the other hand, AC etched (in aqueous solution of NaOH) W has been used as a tip in all the NO and H_2 exposure experiments. After introduction into the microscope, the W tip was sputtered with Ar^+ to remove oxides and other contaminants from the apex of the tip. All STM images have been recorded from top left to bottom right with the fast scan direction from left to right and have been corrected with line-by-line background subtraction and have been analyzed and imaged using Gwyddion [134] and Spacetime [135].

[1] TM Kalrez® 7075 [40]

4.3 Results and discussion

4.3.1 CO oxidation over Pt(110)

Figures 4.1 and 4.2 summarize characteristic STM images obtained during CO oxidation over Pt(110). Figure 4.1 shows three STM images of the Pt(110) surface under different reaction conditions. Figure 4.1a shows the surface in vacuum at room temperature after being transferred to the reactor, and after the coarse approach of the tip. The surface clearly shows a pattern of rows. The distance between these rows is 0.75±0.03 nm determined from the height profile shown in Figure 4.1a, which is in excellent agreement with the theoretical value of the (1×2) missing-row reconstruction of 0.78 nm [133]. Interestingly, in the upper left part of the image the surface deviates from the missing-row pattern and small patches become apparent. At this point, the surface has been exposed to poor vacuum, determined by the outgassing of the reactor walls and seals without being pumped for the time it takes to perform the approach of the tip. Therefore, we attribute the appearance of these patches to the partial lifting of the (1×2) missing-row reconstruction due to adsorption of outgassing molecules.

The sample was heated to 433 K and a flow of a mixture of CO and O_2 (CO/O_2 ratio > 0.2) was introduced at a total pressure of 1 bar. Under these conditions, the STM image shown in Figure 4.1b has been recorded. Excitingly, the high-pressure and elevated temperatures have not significantly deteriorated the imaging quality. The image clearly again shows a row pattern on the two imaged terraces. The distance between these rows corresponds to the (1×1) unreconstructed surface, as can be read off from the height profile in Figure 4.1b. This is the first time that the row structure of this surface has been observed under these reaction conditions. The blurry appearance of the step edge reflects the highly dynamic step fluctuations that are typical, given the high-temperature, high-pressure conditions. To summarize, the high-pressure exposure of the Pt(110) surface to a CO-rich flow lifts the (1×2) missing-row reconstruction and reveals a well-ordered (1×1) structure.

Figure 4.1c shows the sample in an O_2-rich flow with a CO/O_2 ratio of less than 0.2. In this regime, the surface has switched again, this time to a row pattern with a row distance of 0.72±0.06 nm, corresponding to a (1×2) structure. Remarkably, even with the roughness we observed under these conditions, the atomic rows are resolved and they exhibit the same row distance at all height levels.

This (1×2) structure is not a missing-row reconstruction. If it were, one should expect an abrupt increase in roughness, when the surface switches from the (1×1) to the (1×2) structure, since the top layer of Pt atoms in the (1×1) surface contains twice the number of Pt atoms compared to the top layer of the (1×2) missing-row reconstruction. As a result, one should expect that after the transition the surface would exhibit an island and hole pattern of two height levels. This transition-induced roughness would then decay over time. However, this behavior has not been observed. Instead, the opposite was witnessed. Immediately after the switch, there was no increase in roughness, whereas roughness was observed to build up as a function of time after the transition. Figure 4.1c' shows a stage in which significant roughness had been built up already, in the form of protrusions with a height of several nanometers.

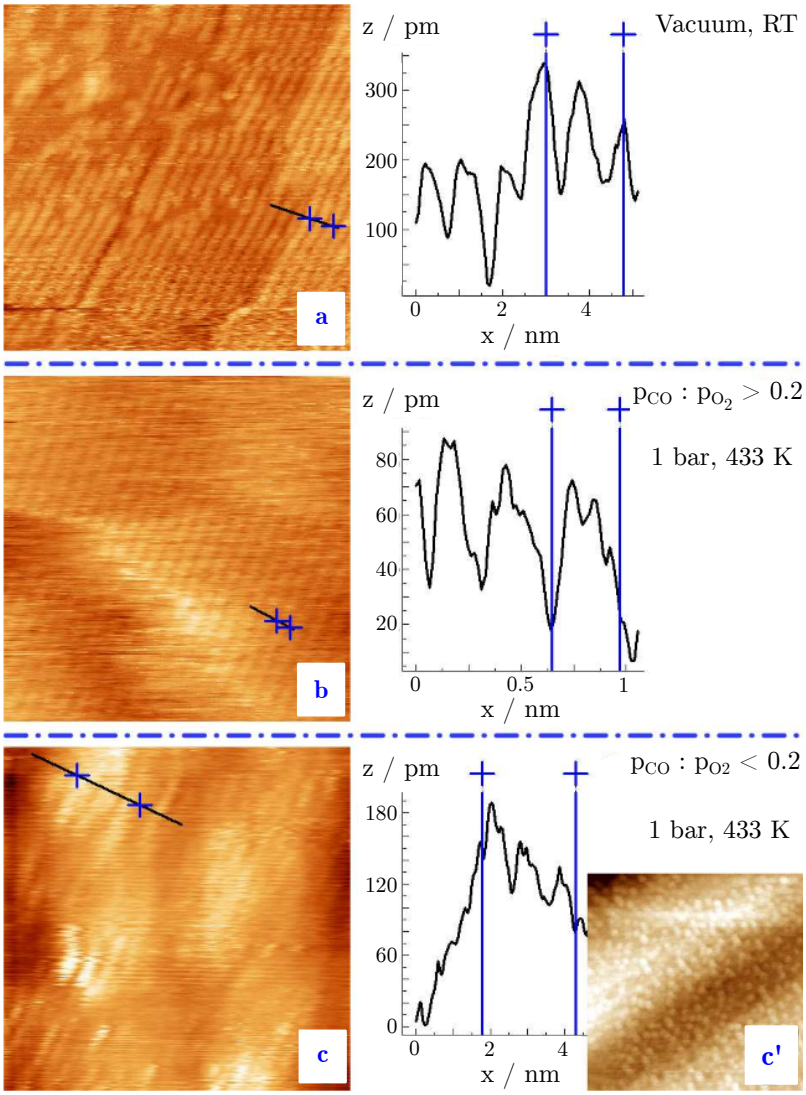

Figure 4.1: STM images and corresponding height profiles obtained with the ReactorSTM during CO oxidation experiments under high-pressure, high-temperature conditions. (a), The missing-row reconstruction, room temperature, vacuum, 25×25 nm^2, U_{bias} = 2.39 V, and I_{tunnel} = 49 pA. Partial lifting of the reconstruction is observable in the top left of the image. (b), the unreconstructed (1×1) surface in CO-rich conditions, 1 bar, 433 K, 7.5×7.5 nm^2, U_{bias} = -0.04 V, and I_{tunnel} = -86 pA. (c), the (1×2) surface oxide in O_2 rich-conditions, 1 bar, 433 K, 12.5×12.5 nm^2, U_{bias} = -0.10 V, and I_{tunnel} = -39 pA. A few bad scan lines due to feedback instabilities have been removed to enhance the image quality. (c'), large scale image of the surface oxide showing the formation of protrusions on the surface as a result of the Mars-van Krevelen-like reaction mechanism, same conditions, 210×210 nm^2 [21].

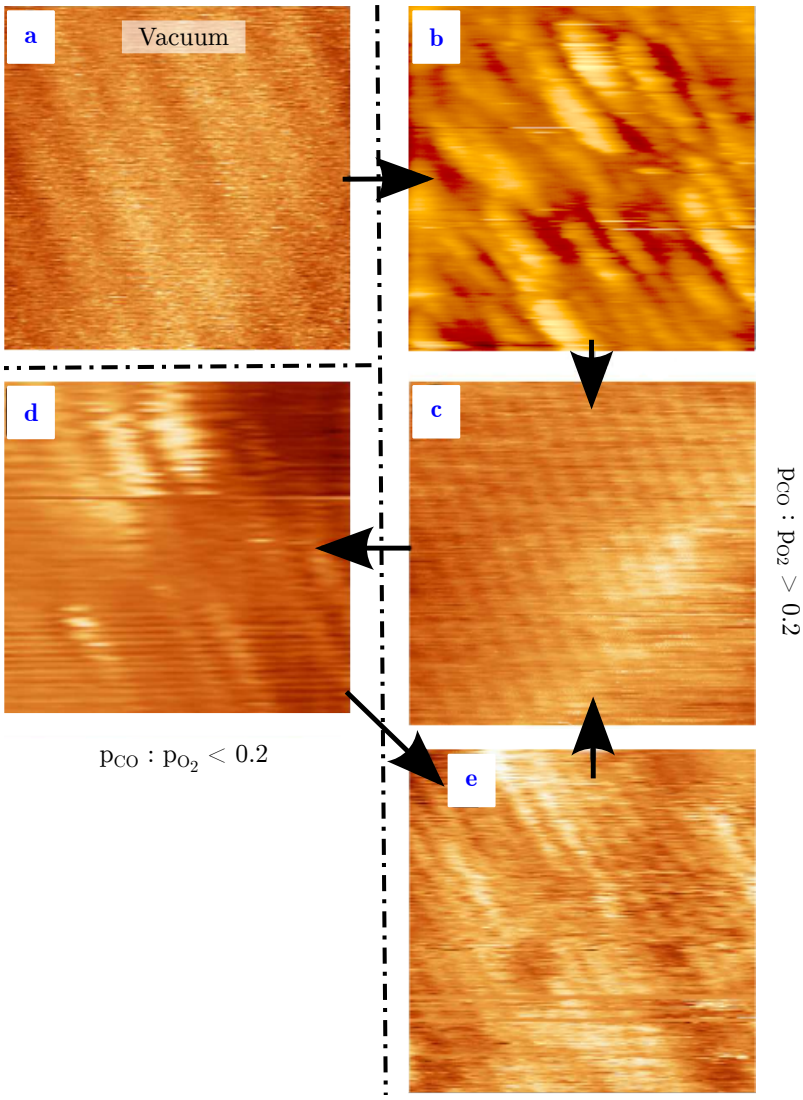

Figure 4.2: STM images obtained with the ReactorSTM demonstrating the development of roughness at various stages of the CO oxidation experiment. (a), missing-row reconstruction, room temperature, vacuum, 4.5×4.5 nm^2, U_{bias} = -0.10 V, and I_{tunnel} = -52 pA. (b), lifting of the reconstruction observed during exposure to 1 bar of CO. Note that the transition from the missing-row reconstructed (1×2) surface to the (1×1) structure has made the surface rough. T = 433 K, 15×15 nm^2, U_{bias} = 0.10 V, and I_{tunnel} = 749 pA. (c), flat (1×1) structure in a CO-rich flow, T = 433 K, 4.5×4.5 nm^2, U_{bias} = -0.04 V, and I_{tunnel} = -86 pA. (d), commensurate (1×2) structure, observed immediately after switching to a more O_2-rich gas mixture. Note that the surface is still relatively smooth. T = 433 K, 4.5×4.5 nm^2. (e), Rough, metallic (1×1) surface, observed after increasing the CO content of the gas mixture again. T = 433 K, 4.5×4.5 nm^2, U_{bias} = 0.08 V, and I_{tunnel} = -1004 pA.

This increased roughness could be attributed to the catalytic reaction taking place under these conditions. Before discussing this mechanism in further detail, we present results of more experiments where we attempted to decouple both mechanisms (decay of the roughness introduced by lifting of the surface reconstruction vs. building up roughness due to the catalytic reactions). We prepared a clean Pt(110) surface, exposed it to a high-pressure CO flow in order to find the initial roughness that is associated with the lifting of the (1×2) missing-row reconstruction and the decay over time. The results of this experiment are shown in Figure 4.2. Figure 4.2a shows the initial (1×2) reconstructed Pt(110) surface, imaged in vacuum. After setting up the CO flow at 1 bar, we find initially increased roughness (Figure 4.2b) which eventually decays, resulting in the flat (1×1) periodicity (Figure 4.2c).

The experiment was continued by adding O_2 to the flow. The (1×1) surface shown in Figure 4.2c changes to the (1×2) structure when the CO/O_2 ratio is decreased below 0.2 (O_2-rich mixture, Figure 4.2d), which corresponds to the conditions of the measurement shown in Figure 4.1c. Because the dimensions of Figures 4.2c and 4.2d are identical, the images can be directly compared and the doubling of the distance between the rows is clearly observable. In Figure 4.2d, there is no immediate increase in roughness, excluding the possibility that this structure reflects the formation of the missing-row reconstruction, as explained above. Prolonged exposure of the sample to O_2-rich conditions results in the increase of roughness over time, which is intimately related to catalytic turnover. This will be further discussed below. The result of this roughening is still present immediately after switching the flow back to CO-rich conditions and the accompanying transition from (1×2) back to (1×1). Under CO-rich conditions (Figure 4.2e) the surface roughness decreases steadily over time to the level of Figure 4.2c.

The nature of the (1×2) structure occurring under reaction conditions at CO/O_2 partial pressure ratios below 0.2 has been studied previously by STM [21], SXRD, and DFT [116]. The STM study suggested the structure to be an oxide, based on a change detected in the electronic structure inferred from scanning tunneling spectroscopy. The SXRD study identified this structure under similar conditions to be a commensurate lifted-row reconstruction in which every second row is lifted, thus giving a (1×2) periodic structure. The lowest energy structure with such lifted rows, found in DFT calculations, was stabilized by a combination of a row of carbonate ions below each lifted Pt row [116]. In addition to pushing the Pt row up, they also displace it sideways, in accordance with the SXRD analysis. In addition, the DFT results indicate the presence of a row of surface oxygen atoms bonding to each lifted Pt row. Combining the results of these studies, it is convincingly shown that this (1×2) structure formed under O_2-rich conditions is a commensurate oxide in which every second row is lifted by the incorporation of carbonate ions. Figures 4.1c and 4.2d represent the first series of STM images in which this (1×2) lifted-row structure, which only appears under these harsh reaction conditions, is resolved in real space.

The increasing roughness under reaction conditions has been measured before on Pt(110) [21] and on Pd(100) [136, 137], and is explained as a side effect of a Mars-Van-Krevelen-like reaction mechanism [138]. In this mechanism, the catalyst plays an even more intimate role than in other reaction mechanisms in heterogeneous catalysis. One of the reactants actually reacts with the catalyst to form a film of what could be

regarded as an intermediate product in the reaction. Subsequently, the other reactant reacts with this intermediate product. In this model catalyst, we have identified the active structure of the catalyst under O_2-rich conditions to be a commensurate surface oxide, as explained above. The oxygen atoms from the oxide layer react with CO to form CO_2, leaving behind reduced and undercoordinated Pt atoms.

Pt atoms that become sufficiently undercoordinated, which probably requires the local loss of two or more oxygen atoms, may be expected to become mobile and diffuse over the surface. These Pt atoms will become immobilized again when they are oxidized by oxygen arriving from the gas phase. This reduction-diffusion-oxidation cycle will enhance the roughness of the surface.

When the CO/O_2 ratio is decreased even further, the hexagonal and incommensurate α-PtO_2 is formed on the surface, as observed with HP SXRD [116]. However, this α-PtO_2 has not been detected in the ReactorSTM, most likely because the CO/O_2 partial pressure ratio could not be lowered far enough in this experiment.

A model summarizing the results of this work, previous STM data, the SXRD data, and the DFT results is given in Figure 4.3. The well-prepared surface in vacuum shows the (1×2) missing-row reconstruction (Figure 4.3a). This reconstruction is lifted in a CO-rich flow, forming a rough (1×1) surface (Figure 4.3b). The roughness is decreasing over time enhanced by the elevated temperature to a well-ordered (1×1) structure (Figure 4.3c). When the composition is changed from CO to O_2 rich, the commensurate surface oxide forms, with the incorporated carbonate ions (Figure 4.3d). The roughness of this oxide increases as a result of the Mars-Van Krevelen-like reaction mechanism (Figure 4.3e). Increasing the CO concentration again reduces the oxide and a rough (1×1) surface is obtained (Figure 4.3f). The rough (1×1) surface smoothens to restore a flat (1×1) surface as depicted in Figure 4.3c. The cycle between Figures 4.3c, 4.3d, 4.3e, and 4.3f could be reproduced many times. A parallel cycle involves the formations of the incommensurate and bulk-like α-PtO_2 at an even lower CO/O_2 ratio. This oxide also roughens through a similar mechanism, only much more slowly because the reaction rate is lower due to the low concentration of CO present. As mentioned already, this α-PtO_2 has not yet been observed in the ReactorSTM.

One of the major advantages of the ReactorSTM over other STM setups able to scan at near-ambient pressures is that we can not only go to higher pressures and temperatures, but also measure the reaction kinetics simultaneously with imaging the surface. The kinetic results for the present study of CO oxidation are presented in Figure 4.4. The most obvious features in Figure 4.4 are the broad peaks in the CO_2 production, when switching back and forth from CO to O_2 rich. These peaks are indicative of LH kinetics in which the reactivity is highest when the CO and O surface coverages are equal. The details in Figure 4.4, however, show more interesting behavior. One feature is the fact that the reactivity of the oxide, which is present under O_2-rich conditions, is higher than the reactivity of the metallic surface, which is present under CO-rich conditions. The other interesting detail is the presence of narrow spikes notable just before the LH peaks in the CO_2 production but only when switching from the oxide to the metallic surface. These spikes are ascribed to the increase in reaction rate when the CO content above the oxide is raised and the sudden drop in reaction when the active surface oxide is removed at the point where

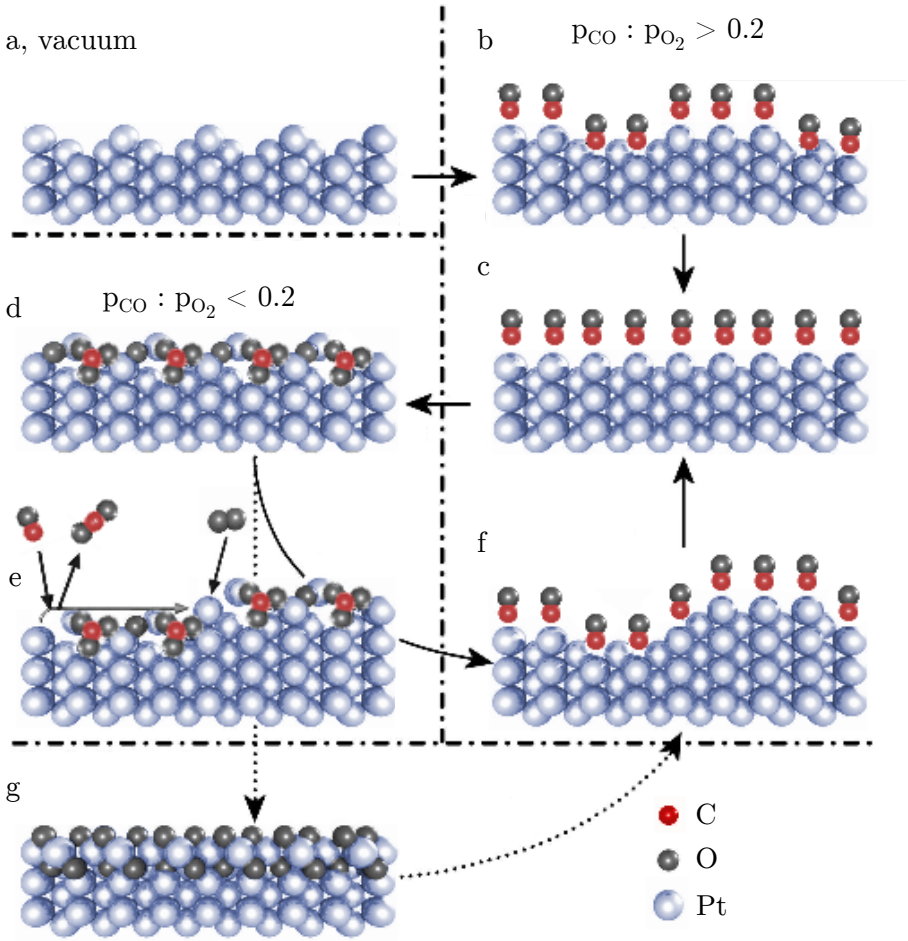

Figure 4.3: A ball model explaining the different transitions observed in studying CO oxidation on Pt(110). (a), shows the missing-row reconstruction in vacuum. This reconstruction is lifted in a CO-rich flow to give a rough (1×1) surface, (b). This roughened surface flattens out with time, (c). When the O_2 content is increased, the commensurate lifted-row oxide is formed, (d). The Mars-van Krevelen-like reaction mechanism increases the roughness over time, (e). Increasing the CO partial pressure results in a rough (1×1) surface, (f), which smoothens over time, (c). At high O_2 partial pressures the incommensurate α-PtO_2 can be formed, (g).

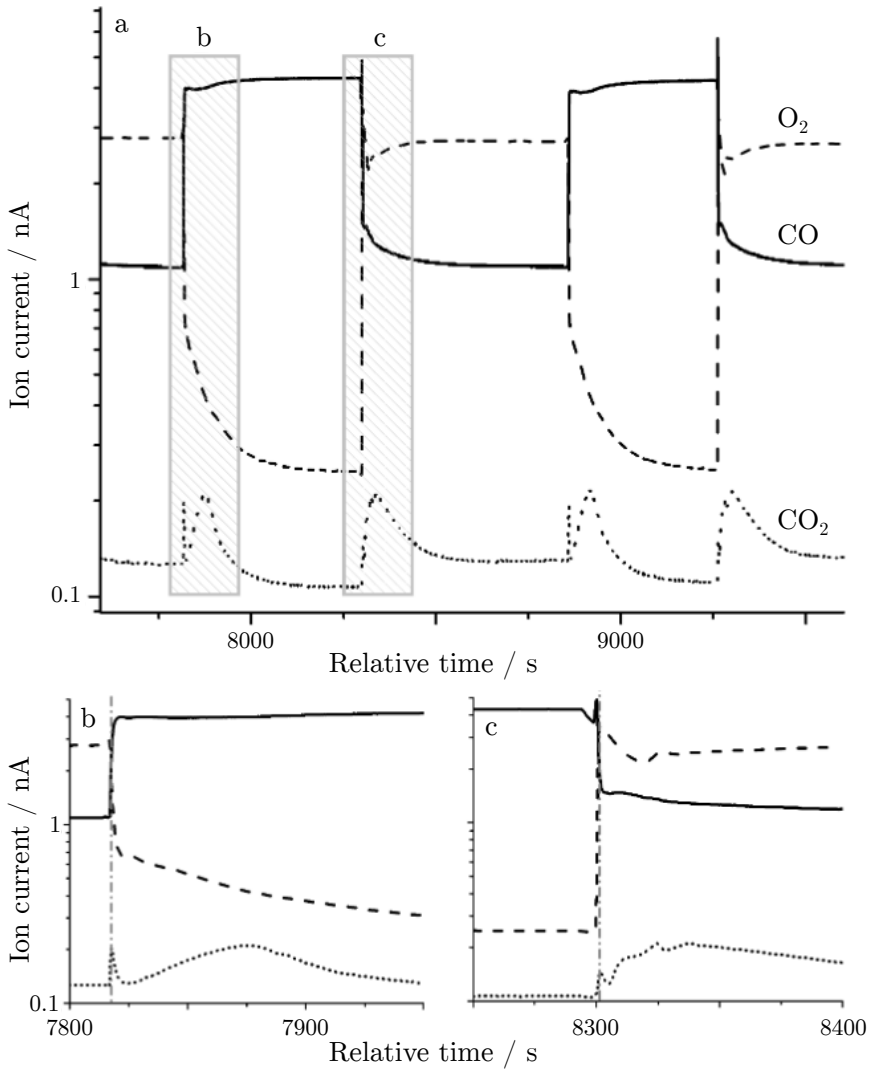

Figure 4.4: Semi-logarithmic plot of the reaction kinetics during CO oxidation, measured with a QMS. The measured ion current is proportional to the partial pressure of the selected mass. (a), two cycles in which the gas composition has been changed back and forth from CO (solid line) to O_2 (dashed line) rich. The product of this reaction, CO_2 (dotted line) shows broad peaks during the switching between the gases that can be explained with Langmuir-Hinshelwood (LH) kinetics. In the case of random adsorption, the maximum of each LH peak corresponds to a situation with equal O_{ad} and CO coverages. (b) and (c), grey dashed regions are replotted on an expanded time scale. The oxide shows higher activity, compare the tails in CO_2 between (b) and (c). The spike in (b) indicates the high reaction rate on the oxide during the initial stage of increase of the CO partial pressure, followed by the drop in the rate, when the oxide is removed due to the high CO partial pressure.

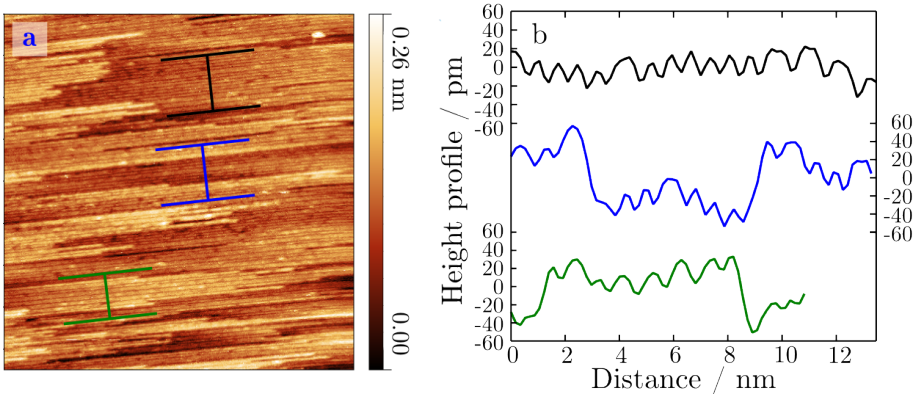

Figure 4.5: (a), STM image, 84×85 nm^2, U_{bias} = -0.70 V, and I_{tunnel} = 121 pA with three height, (b), profiles of Pt(110) obtained with the sample in the closed reactor in vacuum at room temperature prior to the NO reduction experiments.

the CO supply has become too high. To make this effect more visible, Figure 4.4b and Figure 4.4c show two small regions of Figure 4.4a on an expanded time scale.

4.3.2 Exposure to H_2 and NO

The second reaction that we investigate in this chapter, is the reduction of NO by H_2 on Pt(110). This reaction is related to the reduction of NO by CO, which is again one of the important reactions in an automotive catalyst. The nature of this system is more complicated than the oxidation of CO, in which there is only one major reaction with a single product. To reduce NO using H_2 several pathways are possible, creating a combination of NH_3, H_2O and N_2, among others. These products could have a profound influence on the structure of the catalyst. The first stage in our investigation of this reaction system has been to expose Pt(110) to H_2 and NO at high pressure (1.2 bar) at room temperature.

In these experiments, the starting configuration of the Pt(110) surface was less well-ordered than that in the CO oxidation experiments, presented in Figures 4.1a and 4.2a. In Figure 4.5a, an STM image of 84×85 nm^2 is shown. Before this image was measured, the surface was exposed for several minutes to the poor vacuum of the flow reactor cell. In the STM image, it is clearly visible that the surface shows a pattern of rows with a few distinct widths, which we will discuss first.

Figure 4.5a shows three height profiles taken from Figure 4.5a. These height profiles have been averaged over several lines to increase the signal-to-noise ratio. Profile 1 (black) shows predominantly narrow rows with a repeat distance of 0.74 nm. This measured distance corresponds nicely to the (1×2) period of 0.78 nm [133]. In this height profile, several larger periods can be observed of 1.14 nm. The height corrugation of these wider rows is somewhat larger than that for the rows with the

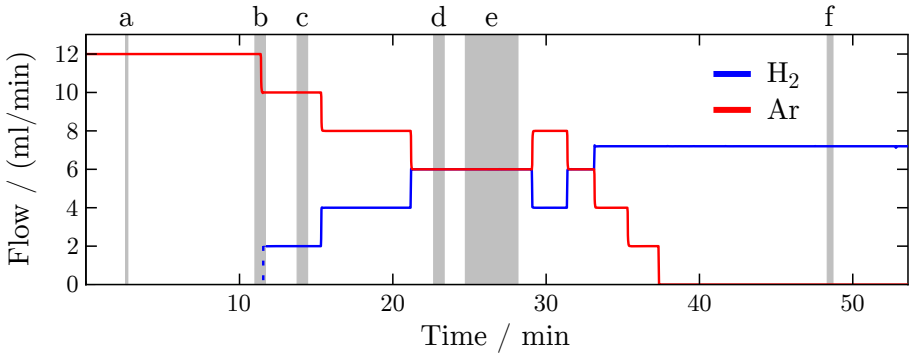

Figure 4.6: Change in gas composition measured as a function of Ar (red) and H_2 (blue) flow rates. The pressure inside the reactor was kept constant at 1.2 bar throughout the entire sequence. Note that the total flow rate (sum of Ar and H_2 flow rates) was varied. The grey regions indicate the time intervals in which the STM images of Figures 4.7 were obtained.

regular (1×2) period. The increase in both width and corrugation suggest that the wider periods are (1×3) missing-row configurations. Profile 2 and 3 (blue and green) in Figure 4.5a also show mixtures of the (1×2) and (1×3) structures and mono-atomic steps on the Pt(110) surface. partial lifting as observed in Figure 4.1a has not been witnessed in the low vacuum of the reactor before the NO reduction experiments. This change with respect to the CO oxidation experiments can be attributed to the increased pumping speed of the reactor before starting the high-pressure experiments.

HP exposure to Ar-H_2 at RT

After the surface had been characterized in the reactor vacuum, a flow of Ar was established at a pressure of 1.2 bar. After setting this flow, the surface was imaged within a minute. After 10 minutes in the Ar flow, the gas composition was changed stepwise from pure Ar to pure H_2 while the surface was imaged with STM. The change of gas composition over time was realized within 30 minutes and is depicted in Figure 4.6. Figures 4.7a and 4.7f show STM images of the surface in pure Ar and pure H_2, respectively. When these images are compared to the image of Figure 4.5a taken in vacuum, an increase in noise is apparent at the higher pressure. This increase could be the result of impurities in the Ar flow that interact with the tip. Nevertheless, we still resolve the atomic rows. In addition to atomic steps, rows within the terraces can be observed.

In Figures 4.7b–e, four STM images are shown for intermediate H_2/Ar gas compositions. Figure 4.7b shows the image in which the gas composition was changed from pure Ar to 1:5 H_2/Ar ratio. Due to the gas flow-induced change in the vertical drift, the height signal of the STM shows precisely at which point in time the surface was confronted with the change in gas composition (see blue dot in Figure 4.7b). This effect remains visible even after line-by-line background subtraction. It is noteworthy that before the gas switch, a tip change occurred in pure Ar. This tip change greatly

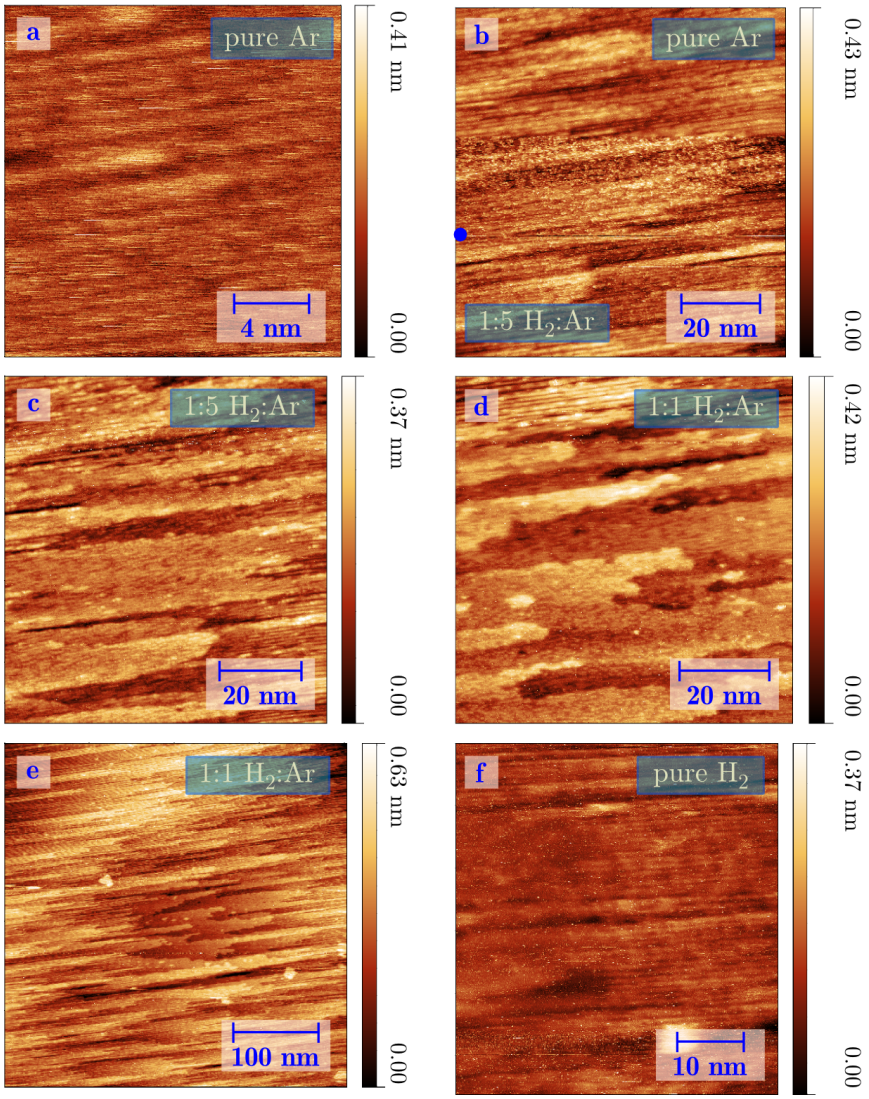

Figure 4.7: STM images obtained with the ReactorSTM during exposure of Pt(110) at room temperature to mixtures of Ar and H_2. (a), surface imaged in pure Ar, 18×18 nm^2, I_{tunnel} = 60 pA. (b), STM image during switch from pure Ar to 1:5 H_2/Ar ratio. The blue dot indicates the scan line of the switch. 84×85 nm^2, I_{tunnel} = 98 pA. (c), 1:5 H_2/Ar ratio, 79×85 nm^2, I_{tunnel} = 165 pA. (d), 1:1 H_2/Ar ratio, 75×82 nm^2, I_{tunnel} = 165 pA. (e), 1:1 H_2/Ar ratio, 403×386 nm^2, I_{tunnel} = 165 pA. (f), pure H_2, 49×56 nm^2, I_{tunnel} = 166 pA. All STM images were obtained at room temperature and with U_{bias} = -0.70 V.

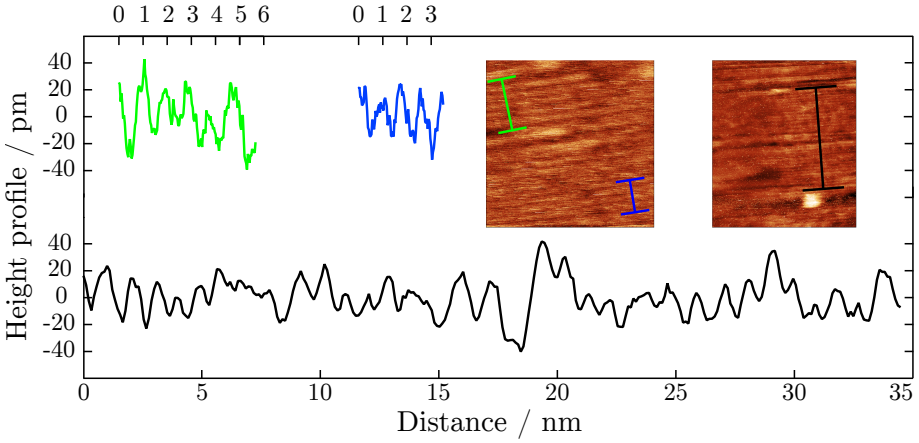

Figure 4.8: Three hight profiles, averaged around zero. Two height profiles (green and blue) were taken from Figure 4.7a and one (black) from 4.7f. The inset shows the STM images with the projection of these height profiles.

enhanced the resolution and some additional internal structure became visible within the atom rows. Figures 4.7d and e show STM images for higher H_2/Ar ratios. The images show a progressive rounding of the steps and a gradual disordering of the missing-row structure. Figure 4.7e is an image that was zoomed out with respect to Figure 4.7d. A mild, rectangular depression can be discerned in the center of Figure 4.7e, corresponding to the scan area of Figure 4.7d and previous STM images. The structure that is visible in this region seems somewhat smoother than that in the freshly scanned region around it. This smooth depression is probably tip-induced and may be indicative of tip-enhanced surface mobility under these conditions. To separate between changes induced by the gas composition and to minimize tip effects, Figure 4.7f was taken in a completely fresh region of the surface. Figure 4.8 shows height profiles taken from Figures 4.7a and 4.7f, which are reproduced in the insets. Two height profiles (green and blue, Figure 4.8) have been taken from the image in pure Ar (Figure 4.7a), and they predominantly show a regular row pattern. The period correspond to the (1×2) missing-row structure with isolated larger periods, most likely (1×3) missing-row configurations, similar to the structure observed in vacuum (Figure 4.5).

The black curve in Figure 4.8 shows the height profile of the image taken in pure H_2. This height line shows structures with both the (1×2) and the (1×3) missing-row periods as well. The observation that both missing-row structures remain intact indicates that the exposure to Ar and (short) exposure to H_2 does not significantly change the surface structure.

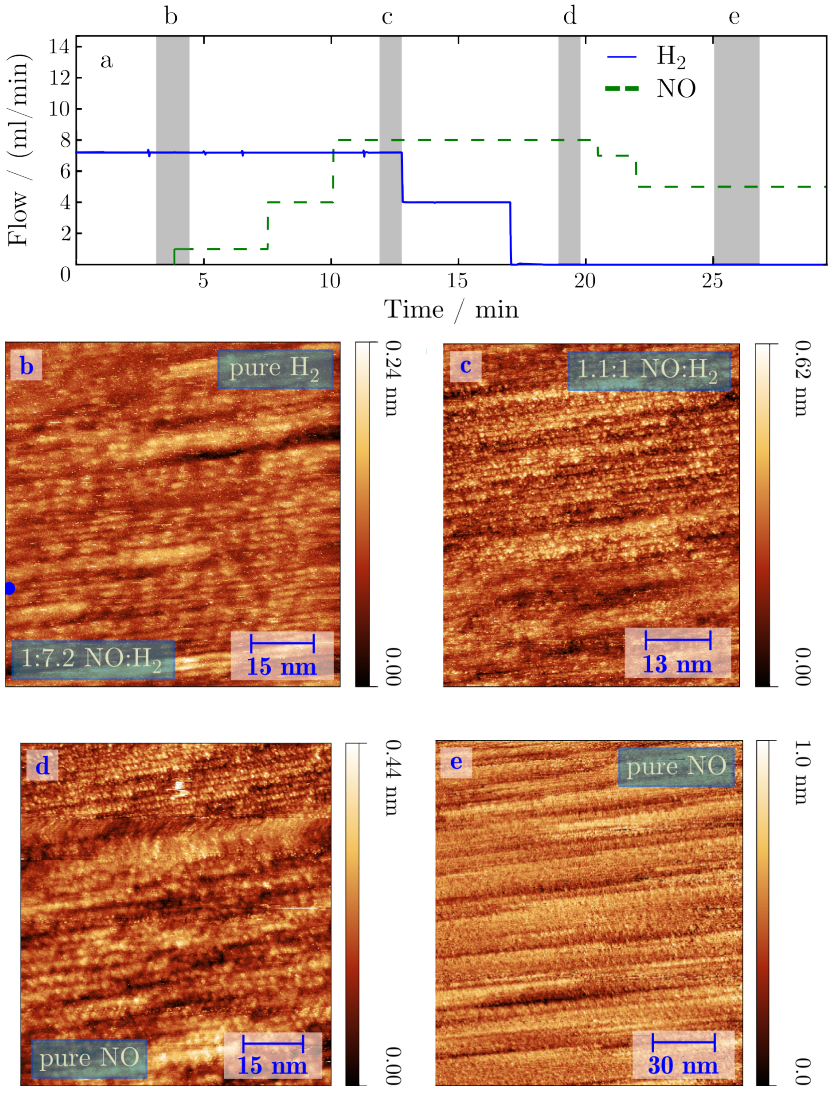

Figure 4.9: Gas composition as a function of time and in situ STM data. (a), shows the stepwise change from H_2 (blue, flow in ml/min) to NO (green, flow set point in ml/min) at room temperature at a constant reactor pressure of 1.2 bar. Grey regions indicate in which time interval and in which conditions the four (b–e) STM images were obtained. (b), surface imaged, while switching from pure H_2 to a mixture with NO, 80×82 nm^2, I_{tunnel} = 139 pA. (c), surface in nearly equal H_2/NO ratio, 73×80 nm^2, I_{tunnel} = 141 pA. (d), sample in pure NO atmosphere, 78×80 nm^2, I_{tunnel} = 141 pA. (e), surface after prolonged NO exposure, 158×160 nm^2, I_{tunnel} = 139 pA. All STM images were obtained with U_{bias} = -0.70 V. STM images recorded in NO flow show frequent tip changes to a state with strongly enhanced resolution.

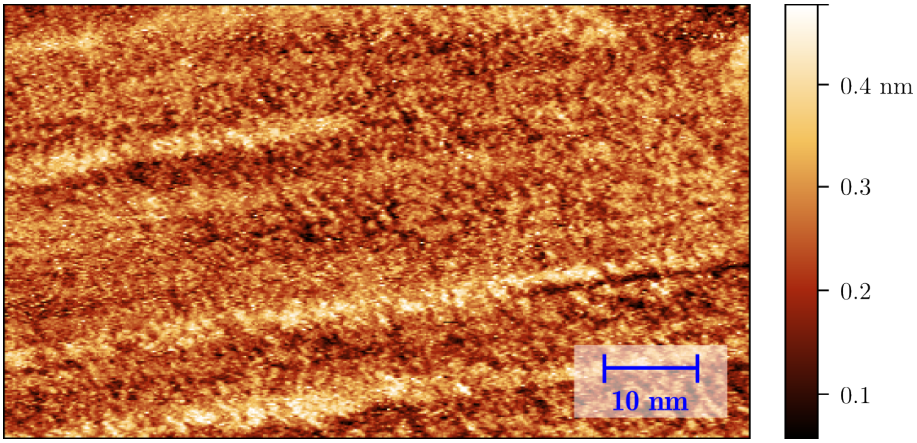

Figure 4.10: Enlarged view of selected region out of an STM images measured in a pure NO flow at room temperature showing enhanced resolution after a tip change. 77×45 nm^2, U_{bias} = -0.70 V and I_{tunnel} = 140 pA.

HP exposure to H_2-NO at RT

Prolonged exposure of the Pt(110) surface (48 minutes after the H_2 was first introduced) to H_2 at 1.2 bar at RT, resulted in a row structure, identified to have a (1×4) periodicity. Also, some deeper missing rows can be observed (Figure 4.9b). The (1×4) reconstructed surface has been exposed to NO at increasing NO/H_2 ratios, see Figures 4.9c–e. Figure 4.9a shows the gas composition as a function of time. During each change of gas composition, the surface was continuously imaged. The blue dot in the first image indicates the switching point from pure H_2 to an NO/H_2 ratio of 0.14. In general, the imaging quality seems to deteriorate only slightly when switching from H_2 to the more reactive NO. This observation is rather remarkable since the material of the tip was W and this is not known as a particularly noble metal. Tip changes are visible in Figures 4.9c and 4.9d, some of which temporarily enhance the imaging resolution significantly. Features of one to several pixels can be distinguished with very high contrast. In both images a single pixel corresponds to 0.21 nm, slightly smaller than the distance between neighboring Pt atoms (0.28 nm [139]). Figure 4.10 shows a selected region from an STM image taken directly before Figure 4.9e in a pure NO atmosphere. This region exhibit enhanced resolution and the row structures can be seen to have disappeared. Directly after the acquisition of this image, the scan region was zoomed out a factor two to check for tip effects, see Figure 4.9e. Although the resolution in Figure 4.9e is not as high as that in Figure 4.10, no tip effect is identified and the loss of the row structure is observed to have occurred also outside of the previously scanned area.

Figures 4.9 and 4.10 demonstrate that when surface and tip are exposed to a gas flow that contains NO, frequent tip changes occur that often lead to a significant improvement in imaging resolution. This effect could be caused by the adsorption of NO on the tip apex, thereby changing the tunneling characteristics. Functionalizing

STM tips to improve resolution or to give chemical contrast in STM images has been achieved before with CO [140, 141], S [142], H_2 [143], and O_2 [144].

Currently, We are investigating the H_2- and NO-induced structural changes of the Pt(110) surface at elevated temperatures, which appear to be more dramatic than the rearrangements reported here for room temperature. These higher temperature observations are complemented with measurements of the reaction rates, e.g., by measuring the partial pressure of the N_2 that is produced, as we illustrated in Figure 4.4 for the CO oxidation reaction on the same surface. These higher temperature experiments will form the subject of a future publication.

4.4 Conclusions

In this chapter, we have presented the first results obtained with the ReactorSTM, a setup combining STM with a flow reactor cell. This system was used to study two highly interesting catalytic reaction systems, namely CO oxidation and NO reduction, both on the Pt(110) surface. Under CO oxidation conditions, we have shown that this surface can adopt different structures. The (1×2) missing-row reconstruction exhibited by a clean Pt(110) surface, is lifted under reaction conditions. At high CO partial pressure, the surface shows an unreconstructed Pt(110)-(1×1) structure. At lower CO/O_2 partial pressure ratios, the surface transforms into a (1×2) surface oxide. Previous STM, SXRD and DFT studies have identified this oxide as a lifted-row configuration, stabilized by the incorporation of rows of carbonate ions and oxygen atoms [116]. In this chapter, we have presented the first STM images, in which the atomic rows of this structure are resolved. In addition, we measured an increased catalytic activity of the surface oxide compared to the metallic (1×1) surface. This higher activity reflects an alternative reaction pathway of the Mars-Van-Krevelen type. We have also observed that this reaction leads to the build-up of surface roughness. The α-PtO_2 structure, that was identified with SXRD under even more O_2-rich conditions was not observed in the present STM study, possibly because the CO/O_2 partial pressure ratio has not reached sufficiently low values in this experiment.

To acquire more insight into the reduction of NO, another important reaction in heterogeneous catalysis, we have studied the structural changes of the Pt(110) surface as a function of NO and H_2 partial pressure. Prolonged H_2 exposure produced both a (1×4) missing-row configuration and some deeper nested missing rows. NO exposure of this surface slowly lifted the surface reconstruction and the row pattern disappeared, leaving flat terraces on the surface. Remarkably, the W tip was relatively stable in the corrosive NO atmosphere. Even more interestingly, the tip frequently switched into a state with significantly improved imaging resolution under NO-rich conditions.